# Transcriptomic Time Series Analysis in Wound Healing: Challenges and Perspectives on Data Interpretation

**Ksenia Zlobina** ( kzlobina@ucsc.edu )
University of California, Santa Cruz
**Eric Malekos**
University of California, Santa Cruz
**Han Chen**
University of California, Santa Cruz
**Marcella Gomez**
University of California, Santa Cruz

**Research Article**

**Keywords:** Transcriptomic time series analysis, wound healing, data interpretation

**Posted Date:** October 6th, 2021

**DOI:** https://doi.org/10.21203/rs.3.rs-929173/v1

# Transcriptomic time series analysis in wound healing: challenges and perspectives on data interpretation

K. Zlobina*, E. Malekos, H. Chen, M. Gomez

University of California, Santa Cruz

*Corresponding author

**Abstract**

**Background:** Wound transcriptomic analysis can be used to quantify wound healing stages and identify leverage points for wound healing intervention. However, individual gene signatures corresponding to wound healing stages vary from one experiment to another and are highly dependent on both experimental setup and bioinformatics methods.

**Methods:** We develop a systematic approach to informatively compare time series from publicly available wound transcriptomic datasets, including mouse and human wounds, and identify consistent gene expression patterns.

**Results:** We reveal the limitations of gene expression data collection, interpretation, and comparison. For example, the sample rate of wound transcriptomic sample collection must be higher than the rate of changes in the wound healing processes, otherwise, important changes in gene expression may be missed. This may lead to mis finding the most significant genes, as peaks of expression for highly differentially expressed genes are lost. Nevertheless, we derived a short list of genes highly differentially expressed in all datasets under consideration. After

clustering and normalization, these genes clearly demonstrate similarly changing dynamics of expression between the wounds and may be used for wound healing stage detection.

**Conclusions:** A list of genes that may be used for transcriptomics-based wound healing stage detection is provided. In addition, we suggest experimental approaches that could help researchers to extract more meaningful results.

## Introduction

Wound healing is a dynamic process involving a series of coordinated biological processes partitioned by scientist into four distinct stages [Canedo-Dorantes 2019]: hemostasis, inflammation [Kim, 2008; Krzyszczyk, 2018], proliferation and remodeling [Bainbridge, 2013; Pastar, 2014]. Many cell types participate in wound healing [Wilkinson 2020], giving rise to expression of different genes [Brant 2015; Deonarine 2007].

Transcriptome microarrays detect expression of tens of thousands of genes. [Blumenberg 2019; Tachibana 2015]. Transcriptomic analysis of cutaneous wound biopsies is particularly promising because the rapidly changing wound environment produces many activation stimuli that induce cellular activation reactions that are not fully understood [Deonarine 2007; Chen 2010]. Until now, only a few experiments with skin wound transcriptomic analysis have been done [GSE460, GSE8056, Greco 2010, GSE23006, Chen 2010].

Despite differences in wound experimental conditions, wound healing stages are assumed to be the same. Thus, common properties of gene expression should exist across wounds. Comparison of transcriptomic data from different wounds was made previously as a

meta-analysis of many datasets from different tissue wounds [Sass, 2018]. The researchers identified several groups of genes that changed expression in most wounds, but not in all.

In this manuscript, we look for genes showing universal expression patterns in different wounds that could serve as wound stage indicators. We restrict ourselves to comparisons between skin wounds. Corresponding datasets are [GSE460, GSE8056, GSE23006] - human and mice burn wounds and mice surgical wounds. For translational work, we present a method to identify patterns in gene expression that are consistent across varying wound experimental conditions and species. This work assess the potential of transcriptomes for data-based predictive models.

To fairly compare across studies, a systematic and consistent approach to identifying differentially expressed genes is applied to all datasets. We identify orthologous genes between mouse and human, only genes with orthologs in all three datasets are considered. We come out with a short list of 58 genes highly differentially expressed in all 3 datasets under consideration. After clustering and normalization, these genes clearly demonstrate similarly changing dynamics of expression between the wounds.

Additionally, we make note of methodological problems in wound transcriptomic analysis and emphasize which shortcomings should be resolved in future experiments to improve the power of this experimental tool for wound investigation.

## Data preparation

Consider 3 transcriptomic datasets from wounds: GSE8056 contains human skin burn wound. GSE460 contains mouse skin burn wound. GSE23006 [Chen 2010] is mouse surgical 1mm wound dataset containing both skin and tongue, of which we consider only the skin data.

To arrive at a list of genetic biomarkers associated with each wound healing stage we search for genes that are reliably highly differentially expressed in all wounds. The following requirements are imposed in our data pre-processing:

- Experimental error must be minimized. That is, we rely on genes with low biological dispersion.
- A link between mouse and human genes must be found.
- To make a direct comparison, each gene must be presented only once in each dataset. All replicates and repeated measurements must be analyzed, and one replicate or mean value accepted.
- Only genes that are present in all datasets may be compared.

To compare gene expression between wounds, we apply several filtering procedures described in “Methods”. The number of genes left in each dataset at each filtering step is presented in Table 1. We emphasize that while we tried to come up with a standardized approach, other approaches can be considered.

***Table 1. Numbers of genes in each dataset after each filtering step (described in Methods).***

| Dataset | GSE23006 | GSE460 | GSE8056 |
|---|---|---|---|

| | mouse skin wound | mouse burn skin wound | human skin wound |
|---|---|---|---|
| Initial number of genes | 45101 | 7275 | 54675 |
| After filtering multiple genes in same row (1) | 29309 | 6130 | 31762 |
| After filtering based on consistency of replicates (2) | 26519 | 5760 | 30242 |
| Unique gene names in filtered subset | 13626 | 4980 | 13777 |
| After filtering of repeated measurements of same gene in each dataset (3) | 8005 | 4449 | 9254 |
| After filtering several genes corresponding to the same homologene number (4) | 7937 | 4441 | 9249 |

84

85

86 **Intersections of filtered datasets**

87 The 3 datasets contain 7937 (GSE23006), 4441 (GSE460) and 9249 (GSE8056) genes after filtering.

88 The intersections contain even less genes, see Table 2.

89

90 ***Table 2. Number of genes in the intersections of each pair of datasets after filtration***

| **Dataset 1** | **Dataset 2** | **N of common genes** |
|---|---|---|
| GSE23006 mouse surg (7937) | GSE460 mouse burn (4441) | 2441 |
| GSE23006 mouse surg (7937) | GSE8056 human (9249) | 5278 |
| GSE460 mouse burn (4441) | GSE8056 human (9249) | 2855 |

Intersection of all 3 datasets consists of 1622 genes.

## Data characterization and comparison

### Fold change as indicator of highly differentially expressed genes

To find the most significant genes, researchers often assign some rank to each gene and select a final gene list based on it. Though not universal [Dalman 2012; McCarthy 2009], in many papers the maximal fold change is used as an indicator. Suppose that gene expression during wound healing is given by a vector of intensities: $\vec{g} = [g(t_0), g(t_1), \cdots, g(t_k)]$ at time points $t_0, t_1, \ldots, t_k$. Then the maximal up- or down-regulation fold change may be found by formulas

$\Delta G_u = \frac{I_{max}}{I_0}$ and $\Delta G_d = \frac{I_{min}}{I_0}$, respectively,

where $I_{max} = max(g(t_i))$, $I_{min} = min(g(t_i))$, and $I_0 = g(t_0)$. Here, we introduce the relative maximum observed fold change

$$\Delta G = \frac{I_{max} - I_{min}}{I_{min}}$$

To account for variations in baseline expressions across datasets. To find common and unique features of the wounds considered, we try to differentiate genes that are commonly differentially expressed in all wounds from those with high variation across wounds. In other words, we ask how many genes have approximately the same value of fold change in all wounds.

Figure 1 shows the distribution of genes by the value of fold change $\Delta G$. As seen from Figure 1, there is no "natural" threshold value for $\Delta G$ to distinguish between differentially expressed genes and non-differentially expressed. The amount of differentially expressed genes fully depends on the researcher's choice of the threshold for $\Delta G$.

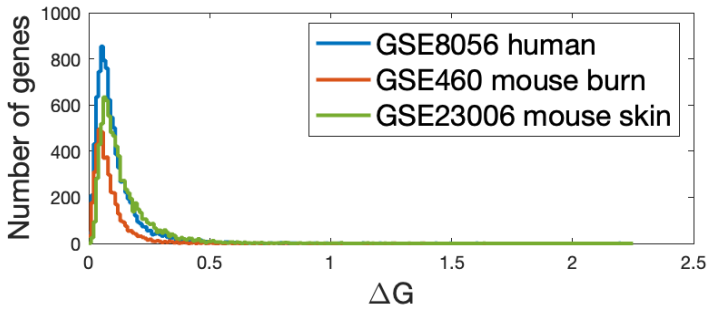


***Figure 1 Distribution of genes by the value of fold change $\Delta G$.***

Figure 2 demonstrates the relation of $\Delta G$ for each gene between datasets. Each gene is presented by one point with abscissa $\Delta G$ from one dataset and ordinate $\Delta G$ from another dataset. One can see that there is no strong correlation of $\Delta G$ between each pair of wounds with Spearman rank correlation coefficients calculated in Table 1.

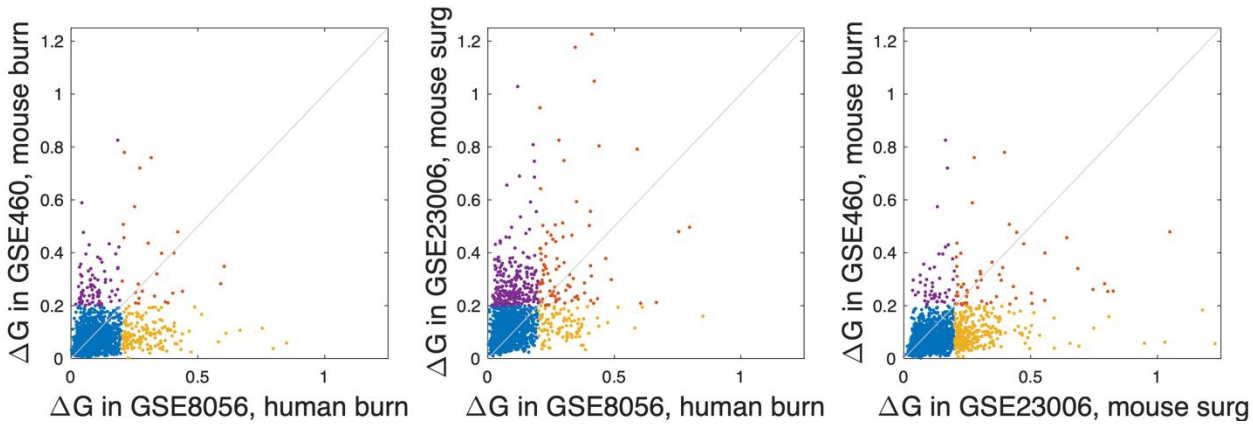


***Figure 2. Comparison of gene fold change $\Delta G$ between datasets for all intersecting genes. Each point corresponds to one of 1622 genes shared by all 3 datasets. Different colors denote genes with $\Delta G$ above (orange) or below (blue) 0.2 in both datasets as well as those with differing fold changes across dataset (purple, yellow).***

***Table 3. Spearman correlation coefficients between datasets calculated by different ranks.***

| Datasets:<br><br>Rank type | mouse surg vs<br>mouse burn | mouse surg vs<br>human | mouse burn vs<br>human |
|---|---|---|---|
| Fold change $\Delta G$ | 0.42 | 0.36 | 0.27 |
| Max upregulation<br>$\Delta G_u$ | 0.39 | 0.34 | 0.22 |
| Max downregulation<br>$\Delta G_d$ | 0.22 | 0.29 | 0.15 |

The distribution of $\Delta G$ is similar for all 3 datasets (Figure 1), however, the correlation between datasets is weak (Table 3), i.e. if the gene has high/low $\Delta G$ in one wound, it does not necessarily imply similar dynamics in another wound (Figure 2).

## Challenges in comparing gene expression dynamics between datasets

Low correlation between gene expression fold change in different datasets may be explained by an inconsistency in measurement time points. Figure 3a shows the dynamics of one gene (Il1a) with different values of $\Delta G$ in 3 datasets; the plots look very different. The mouse surgical wound dataset contains eight timepoints over 10 days, while the mouse burn dataset contains only four timepoints over 14 days. Some genes are upregulated in the early wound healing stages. The mouse surgical wound, which contains measured timepoints between 2 and 72 hours, is able to

capture these early transient dynamics. However, the mouse burn wound does not contain measured timepoints in this time window. Thus, any potential transients would be missed. For example, even if Il1a would have upregulation in this period (dashed plots in Fig. 3b) in burn wounds, similarly to mouse surgical wound, this cannot be seen in the burn wounds.

The same is observed for many other genes; in this work they are filtered out.

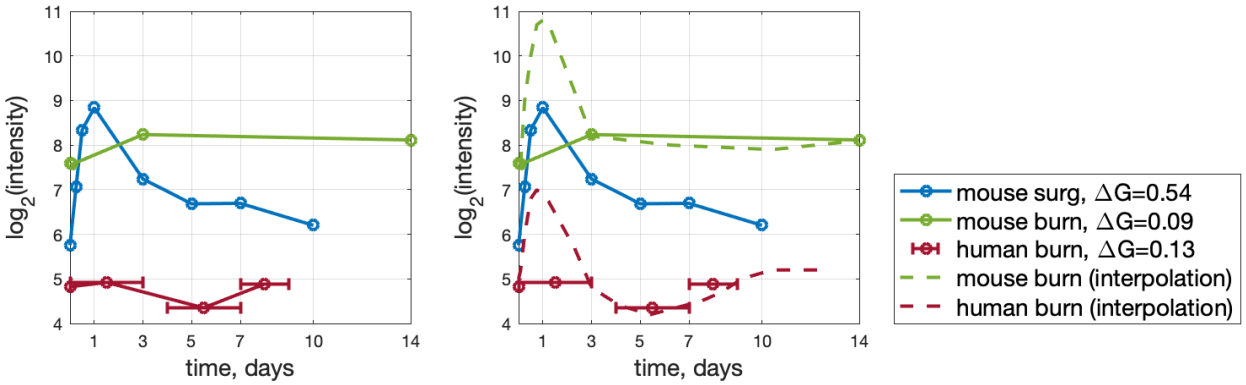


***Figure 3. (a) Plots of Il1a expression change vs time: comparison between wound datasets. (b) The same gene dynamics along with possible gene expression plots (fake plots) corresponding to data but not captured due to lack of time points (dashed line).***

## Commonly highly expressed genes

We search the genes having high $\Delta G$ in each dataset. As described above, there are 1622 genes that appear in all three datasets after filtration. As there is no natural cutoff for $\Delta G$ values (Figure 1) we select the first 300 genes with the highest $\Delta G$ from each dataset. The intersection of 3 subsets of 300 genes is 58 genes only. The plots of these 58 genes' dynamics in 3 wound datasets are presented in Figure 4.

The genes were divided into 5 clusters (see Figure 4) based on the peak time in GSE23006 mouse surgical data, where peak time refers to the window in which $\Delta G$ is maximized. Cluster1

158 includes genes with peak time in mouse surgical wounds equal to 0-12h, Cluster2 – 24h, Cluster3
159 – 72h, Cluster4 – 120h and Cluster5 >120h. Next the plots of the same genes in other datasets
160 were divided into the same cluster as GSE23006 mouse surgical, independently of their dynamics
161 in other datasets.

162 We generally observe similar dynamics for the genes in each cluster. In contrast the
163 clusters for each dataset exhibit different dynamics as can be seen by comparing images on the
164 same row.

165 Compared to the gene dynamics within a cluster, there is less similarity of dynamics
166 between wounds: the same cluster of genes demonstrates only roughly comparable dynamics
167 between the wounds (compare images within the same column). The genes of the first cluster
168 are downregulated from 0 to 72 h in all datasets and genes of the 3$^{rd}$ cluster are mainly
169 upregulated at the same interval. However, if we compare the last cluster of genes, we see early
170 downregulation of genes in the surgical wound that is not mirrored in either of the burn wounds.
171 The unexpected outcome in this latter case may be due to the low-resolution time steps masking
172 the underlying dynamics.

173

174

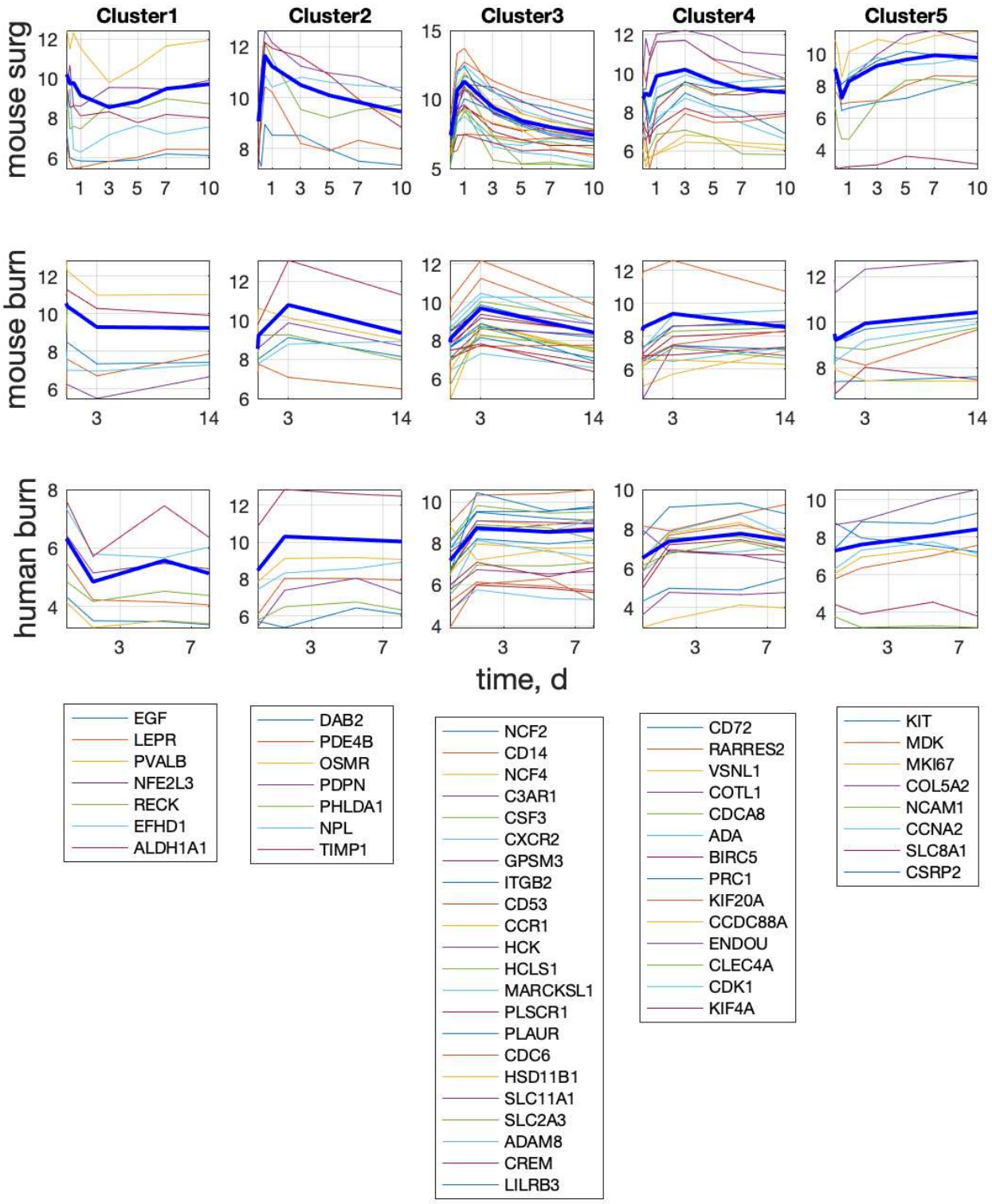


***Figure 4. Gene expression dynamics of commonly highly expressed genes in the 3 datasets. Each row represents the same dataset and each column represents the same cluster of genes listed***

***in the legend under each column. Bold blue line in each plot corresponds to the mean value of gene intensity within each cluster (calculated for each dataset separately). Vertical axis: $log_2$(Intensity), horizontal axis – time in days.***

To finalize comparison of gene expression between the wounds, we normalize the mean cluster value by dividing by its initial value (t=0, non-injured tissue):

$$Normalized\ mean\ cluster\ value = \frac{J_i}{J_0}$$

$$J_i = \frac{1}{N}\sum_k^N g_k(t_i),$$

where summation is over all genes within the cluster and N is number of genes in the cluster.

In Figure 5 normalized mean cluster value dynamics from the 3 datasets is collected.

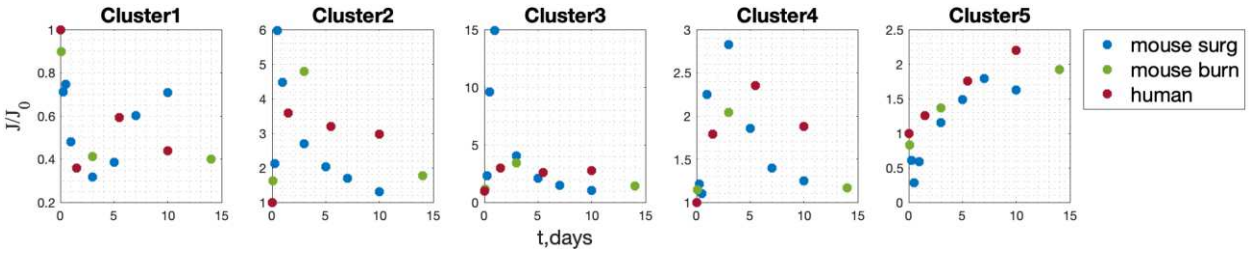


***Figure 5. Normalized mean cluster value dynamics in three wound datasets. Clusters indicated in Fig.4.***

One can see that all five normalized mean cluster gene expression values have very similar dynamics between wound datasets. Thus, we found the set of genes that could be used as universal indicators of wound stage detection in different wounds.

## Discussion

Wound healing, independently of wound origin, is traditionally divided into phases: homeostasis, inflammation, proliferation, and remodeling [Canedo-Dorantes 2019]. Though skin repair in mice does not perfectly mirror that of humans, prior experiments have shown that skin healing is similar in humans and mice [Zomer 2017]. This work supports our assumption that universal features of wound healing may be found even in different wound transcriptomic datasets.

Wound transcriptomic datasets are not numerous. In fact, we have only few wound experiments collected under different conditions [Raudys, 1991]. However, following [Sass 2017], we compared existing wound data, but focused on finding genes with similar dynamics. We found 5 clusters of genes whose dynamics were similar in 3 available datasets. These are strong candidates to universal biomarkers of known wound healing stages.

During our comparison analysis we found several methodological problems that hopefully will be solved in the future.

Wound healing is a dynamical process. Experimental data collection, such as gene expression intensity, should be done with appropriate frequency (sampling rate). In signal processing the theorem of Nyquist-Shannon limits the frequency of discrete sampling to obtain satisfactory information from a continuous signal [Dieter, 1999]. The sampling rate frequency must be twice larger than the highest frequency of the signal. In many existing wound transcriptomic datasets, the sampling rate doesn't satisfy this condition (see Figure 3). Characteristic healing times depend on wound size, depth, experimental conditions, and overall organism's health, etc. [Hess 2008; Canedo-Dorantes 2019; Hadian 2020]. Wound

transcriptomics experiments are expansive and raise ethical questions, however, sampling rate frequency must be taken into account when planning such experiments.

It is traditional in this field to assume high fold change in gene expression as high significance of the gene. However low sample rate may lead to missing gene expression peak (burn wounds in Fig 3) and misinterpretation of its significance. On the other hand, in the fold-change values of genes there is no “bi-modal” distribution (highly changing and no-changing dynamics) (Figure 1). Whether or not two-fold change or three-fold change expression is considered significant is an arbitrary choice of the researcher. If high fold change is equivalent to the “significance”, then the significance of genes decreases gradually, there are no “significant” and “non-significant” genes. Probably, the choice of the first N genes with the highest fold-change in expression is more reasonable option to select the most significant genes.

The development of transcriptome technology is important for understanding wound healing and for the improvement of intelligent methods of wound treatment. However, much work is still to be done. For instance, transcriptomic data are usually not accompanied by additional data, such as histology/morphology of the wound tissue. In fact, transcriptomic signals are taken from many cells at once, and any information about the cell types in the wound at each time would give much more insight into understanding of gene expression in wound healing.

In this work we performed wound transcriptomic dataset comparisons without any reference to cells or biological processes and found a set of 58 genes that could serve as indicators of wound healing stage. We used a filtering approach which allowed for comparisons between species and was agnostic to experimental set up. The results were a set of 58 genes

which may be used as a basis for future analysis. Potentially this set of biomarkers, or an improved set pending further data collection and analysis, can be used in biomarkers toolkit for gene-expression based wound stage detection.

## Methods

In each dataset the intensity of gene expression is measured at multiple time points. In GSE23006 the intensities are represented as log2(intensity) while in GSE460 and GSE8056 datasets original intensities are shown. To make datasets comparable, we return GSE23006 to initial intensity before filtering by taking power of 2 of the numbers represented in the GSE23006 array.

**Orthologous genes between mouse and human**

To compare particular genes between human and mouse, we find orthologs - homologous genes between species. All orthologous genes in mouse and human were matched by gene symbol to their homologene ID in *the Human and Mouse Homology Class report*. (Source: http://www.informatics.jax.org/homology.shtml).

The genes are considered for further analysis only if orthologs are found in all datasets under consideration.

**Filtering Data of multiple genes in the same row (1)**

Although most probes in microarray transcriptomics exhibit a one-to-one mapping of probe-to-transcript, this is not always the case. Similarities between the nucleotide sequences of different genes can result in non-unique mappings, witnessed in the form “gene1//gene2//gene3” in the datasets. To avoid faulty comparisons, we simply remove these rows from analysis.

**Filtering Data Based on consistency of replicates (2)**

In all considered datasets each of n genes is presented as 3 replicates in m time points. We first denote the time points by $t_j$ such that $j = 0, \dots, m-1$, where the unwounded state is associated with $j = 0$. Let $G^k$ be an Rnxm matrix composed of m time series gene intensity measurements for kth replicate of each of n genes. Let the average gene intensity across the three replicates be given by

$$G = \frac{\sum_{k=1}^{3} G^k}{3} \in R^{n \times m}$$

Where the division operator is applied component wise. Then the percent relative error for each replicate is given by

$$S^k = \frac{|G^k - G|}{G} * 100 \ \in R^{n \times m},$$

with component wise operation in the division. Next we want to find the average relative error for each time point across all genes and its standard deviation. This gives a sense of how much each replicate deviates from the average across the replicates independent of the gene. Let the matrix

$$S = [S^1 \ S^2 \ S^3 \ ] \in R^{3n \times 8}$$

be a matrix composed of the matrices $S^k$. Then we take the average across the columns such that we arrive at a row vector where each entry $i$ contains the average value across all elements in column $i$ of matrix $S$. We denote this vector by $\vec{r}_{AVG} \in R^{1 \times 8}$ Similarly, we compute the standard deviation across the columns of $S$ and denote this vector by $\vec{r}_{STD} \in R^{1 \times 8}$.

Now we compute the threshold for the maximum relative error, which will determine which data is kept and which is discarded based on an acceptable value for relative error. The threshold for each time point is chosen to be as follows

$$\vec{r}_{Thres} = \vec{r}_{AVG} + 4\vec{r}_{STD}$$

where we take four standard deviations above the mean which is inclusive of 99.98% percent of data assuming a normal distribution (Note that three standard deviations is inclusive of 99.72%). We find the maximum relative error across the three samples, where the new matrix $S_{max} = max(S^1, S^2, S^3) \in R^{n \times m}$. The maximum is taken element wise across the three matrices, that is $S_{max}(i,j) = max(S^1(i,j), S^2(i,j), S^3(i,j))$ and do an element-wise comparison across each row

$$S_{max,(i,:)} > \vec{r}_{Thres}$$

for $i = 1{:}\, n$ and any time-series containing an extreme outlier in any of the replicates at any time point is removed from the dataset and, hence, the row removed from matrix $G$ containing the average intensity across the replicates. Note that we treat each time-point individually since there may exist different degrees of variability through the different wound healing stages. We denote the new matrix $\hat{G}$, which contains a subset of the rows of $G$ , after discarding rows with high variability across replicates.

**Filtration of repeated measurements of same gene in each dataset (3)**

Some genes are mentioned in the dataset several times (several repetitions or several transcripts). In addition, for some genes the repeated rows contain too different dynamics. To leave "one gene – one row" we make filtering based on correlation between repeated gene rows.

Denote the i[th] row of the matrix $\hat{G}$ as $\vec{g}_i \in R^{1\times m}$. It contains time point mean intensity measurements of gene $i$ such that: $\vec{g}_i = [g_i(t_0), g_i(t_1), \cdots, g_i(t_m)]$. Suppose that there are $k$ vectors corresponding to one and the same gene:

$\vec{g}_{i_1}$, …, $\vec{g}_{i_k}$

First, we find Pearson correlation coefficients between each pair of repeated gene intensities: $C_{nm} = corr(\vec{g}_n, \vec{g}_m), n \neq m$, we obtain $k^2 - k$ correlation coefficients. The gene is kept for further analysis if at least two repetitions are highly correlated:

$$(C_{nm}) \geq C \qquad (*)$$

In this work we use the threshold $C = 0.9$. If the condition (*) is satisfied, we take one of highly correlated gene intensity rows $\vec{g}_n$, $\vec{g}_m$ (we can take the mean between the intensities of two highly correlated genes). If the condition (*) is not satisfied, the gene is not included in further analysis.

**Several genes corresponding to the same homologene number (4)**

For some genes it may happen that the same homologene number corresponds to two genes. For example, homologene number corresponding to gene X in mouse corresponds to genes X1 and X2 in human. In this case we check if there is high correlation between homologenes X1 and X2 ($corr(\vec{g}_{X_1}, \vec{g}_{X_2}) > C$) and take one of them. Otherwise, these homologenes are not included in further analysis.

## Declarations

**Ethics approval and consent to participate**

All procedures were performed in accordance with relevant guidelines.

## Consent for publication

Not applicable.

## Availability of data and materials

Publicly available datasets used in this work: GSE23006, GSE460 and GSE8056 from Gene Expression Omnibus database: https://www.ncbi.nlm.nih.gov/geo/

The filtered data created during the current study available from the corresponding author on reasonable request.

## Competing interests

The authors declare no competing interests.


## Funding

Research was sponsored by the Office of Naval Research and the DARPA Biotechnologies Office (DARPA/BTO) and was accomplished under Cooperative Agreement Number DC20AC00003. The views and conclusions contained in this document are those of the authors and should not be interpreted as representing the official policies, either expressed or implied, of the Office of Naval Research and the DARPA Biotechnologies Office (DARPA/BTO) or the U.S. Government. The U.S. Government is authorized to reproduce and distribute reprints for Government purposes notwithstanding any copyright notation herein.


## Authors' contributions

EM, KZ and MG developed the methods and drafted the manuscript. KZ performed data analysis. MG guided the work. All authors discussed, read, revised, and approved the final manuscript.


## Acknowledgements

Not applicable.

## References


1. L.Canedo-Dorantes, M. Canero-Ayala, Skin Acute Wound Healing: A Comprehensive Review // International Journal of Inflammation Volume 2019, Article ID 3706315.
2. M.H. Kim, W. Liu, D.L. Borjesson, F.R. Curry, L.S. Miller, A.L. Cheung, F.T. Liu, R.R. Isseroff, S.I. Simon, Dynamics of neutrophil infiltration during cutaneous wound healing and infection using fluorescence imaging, J Invest Dermatol 128(7) (2008) 1812-20.
3. P. Krzyszczyk, R. Schloss, A. Palmer, F. Berthiaume, The Role of Macrophages in Acute and Chronic Wound Healing and Interventions to Promote Pro-wound Healing Phenotypes, Front Physiol 9 (2018) 419.
4. P. Bainbridge, Wound healing and the role of fibroblasts, J Wound Care 22(8) (2013) 407-8, 410-12.
5. I. Pastar, O. Stojadinovic, N.C. Yin, H. Ramirez, A.G. Nusbaum, A. Sawaya, S.B. Patel, L. Khalid, R.R. Isseroff, M. Tomic-Canic, Epithelialization in Wound Healing: A Comprehensive Review, Adv Wound Care (New Rochelle) 3(7) (2014) 445-464.
6. H.N. Wilkinson, M.J. Hardman, Wound healing: cellular mechanisms and pathological outcomes, Open Biol 10(9) (2020) 200223.
7. J.O. Brant, M.C. Lopez, H.V. Baker, W.B. Barbazuk, M. Maden, A Comparative Analysis of Gene Expression Profiles during Skin Regeneration in Mus and Acomys, PLoS One 10(11) (2015) e0142931.
8. K. Deonarine, M.C. Panelli, M.E. Stashower, P. Jin, K. Smith, H.B. Slade, C. Norwood, E. Wang, F.M. Marincola, D.F. Stroncek, Gene expression profiling of cutaneous wound

healing, J Transl Med 5 (2007) 11.

9. Blumenberg M. Introductory chapter: transcriptome analysis. In: Transcriptome Analysis. Blumenberg M (Ed.). IntechOpen, London, UK, 1–5 (2019).
10. C. Tachibana, Transcriptomics today: Microarrays, RNA-seq, and more. // Science 2015: Vol. 349, Issue 6247, pp. 544-546.
11. L.Chen, Z.H.Arbieva, S.Guo, P.T. Marucha, T.A. Mustoe, L.A. DiPietro, Positional differences in the wound transcriptome of skin and oral mucosa // BMC Genomics 2010, 11:471
12. Greco JA 3rd, Pollins AC, Boone BE, Levy SE et al. A microarray analysis of temporal gene expression profiles in thermally injured human skin. Burns 2010 Mar;36(2):192-204.
13. P.A. Sass, M. Dabrowski, A. Charzynska, P. Sachadyn, Transcriptomic responses to wounding: meta-analysis of gene expression microarray data. // BMC Genomics, 2017, V 18: 850.
14. J. Xue, S.V. Schmidt etc.,Transcriptome-Based Network Analysis Reveals a Spectrum Model of Human Macrophage Activation // Immunity. 2014 Feb 20; 40(2): 274–288.
15. Y.Du, P.Ren. Q.Wang, S.-K. Jiang, M.Zhang, J.-Y. Li, L.-L. Wang, D.-W. Guan, , Cannabinoid 2 receptor attenuates inflammation during skin wound healing by inhibiting M1 macrophages rather than activating M2 macrophages // Journal of Inflammation (2018) 15:25
16. S. Raychaudhuri, J.M. Stuart, R.B. Altman, Principal component analysis to summarize microarray experiments: application to sporulation time series. // Pac Symp Biocomput, 2000, 455-66.

17. A.L. Tarca, R. Romero, S. Draghici, Analysis of microarray experiments of gene expression profiling. // Am J Obstet Gynecol. 2006, 195(2): 373–388.
18. S.J.Raudys, A.K.Jain, Small sample size effects in statistical pattern recognition: recommendations for practitioners. // IEEE Transactions on pattern analysis and machine intelligence, V 13 N 3 1991:252-264.
19. L.H. Dieter, "The Origins of the Sampling Theorem". 1999, IEEE Communications Magazine. 37 (4): 106–108.
20. Hess CT. Clinical Guide to Skin and Wound Care. 6th ed. Philadelphia, PA: Lippincott Williams & Wilkins; 2008.
21. Y. Hadian, D. Fregoso, C. Nguyen, M.D. Bagood, S.E. Dahle, M.G. Gareau, R.R. Isseroff, Microbiome-skin-brain axis: A novel paradigm for cutaneous wounds, Wound Repair Regen 28(3) (2020) 282-292.
22. JL Martin, L Koodie, AG Krishnan, R Charboneau, RA Barke, S Roy, Chronic Morphine Administration Delays Wound Healing by Inhibiting Immune Cell Recruitment to the Wound Site// The American Journal of Pathology 2010
23. L. Chen, S. Nagaraja, J. Zhou, Y. Zhao, D. Fine, A.Y. Mitrophanov, J. Reifman, L.A. DiPietro, Wound healing in Mac-1 deficient mice, Wound Repair Regen 25(3) (2017) 366-376.
24. Evans TG. Considerations for the use of transcriptomics in identifying the 'genes that matter' for environmental adaptation. J Exp Biol. 2015 Jun;218(Pt 12):1925-35. doi: 10.1242/jeb.114306. PMID: 26085669.
25. Feder ME, Walser JC. The biological limitations of transcriptomics in elucidating stress and stress responses. J Evol Biol. 2005 Jul;18(4):901-10. doi: 10.1111/j.1420-

9101.2005.00921.x. PMID: 16033562.

26. Dalman, M.R., Deeter, A., Nimishakavi, G. et al. Fold change and p-value cutoffs significantly alter microarray interpretations. BMC Bioinformatics 13, S11 (2012). https://doi.org/10.1186/1471-2105-13-S2-S11
27. McCarthy, Davis J, and Gordon K Smyth. “Testing significance relative to a fold-change threshold is a TREAT.” Bioinformatics (Oxford, England) vol. 25,6 (2009): 765-71. doi:10.1093/bioinformatics/btp053
28. Zomer HD, Trentin AG. Skin wound healing in humans and mice: Challenges in translational research. J Dermatol Sci. 2018 Apr;90(1):3-12. doi: 10.1016/j.jdermsci.2017.12.009. Epub 2017 Dec 26. PMID: 29289417.